Photoemission spectra and band structures of *d*-band metals. II. Experiments on Rh, Ir, Ni, Pd, and Pt

Morton M. Traum and Neville V. Smith
Bell Laboratories, Murray Hill, New Jersey 07974
(Received 21 May 1973)

Measurements of the photoelectron energy spectrum and its second derivative are reported for Rh, Ir, Ni, Pd, and Pt in the photon energy range $\hbar\omega = 4$ to 11 eV. Experiments were performed on clean samples, prepared by electron-bombardment evaporation, and on cesiated samples. The results on the different metals are compared with each other and with measurements on Cu, Ag, and Au. Relying primarily on the derivative spectra taken on cesiated samples, it is found that the variation of the profile of the spectrum with $\hbar\omega$ displays a consistent pattern from metal to metal. The pattern for one metal is obtained from that of the next by a uniform shifting and stretching of the electron energy scale, thus providing direct experimental support for the resonance picture of the *d*-band metals. The emergence at certain photon energies of some of the peaks in the *d*-band region of the spectra is attributed to the onset of transitions to the unoccupied seventh band. From this it is estimated that the plane-wave-like level L_1 is situated at 5.7, 4.3, 8.5, 8.0, 7.1, 6.1, and 3.6 eV above the Fermi level in Ni, Cu, Rh, Pd, Ir, Pt, and Au, respectively. An energy range in Ir and Rh where direct transitions are forbidden, but photoelectrons are observed, is discussed.

I. INTRODUCTION

In this second paper of the series,[1] we report the results of extensive measurements of the photoelectron energy spectra on the fcc transition metals Rh, Ir, Ni, Pd, and Pt in the photon energy range $4 < \hbar\omega < 11$ eV. The experiments were performed on both clean and cesiated samples. Results have been reported previously for clean samples of all these metals[2-9] except for Ir. Our own experiments on clean samples have reproduced the more definitive of these results[2-6] and we will, therefore, not present them in detail. Our main contribution here lies in the fact that we have had success in cesiating these metals and thus opened up a new energy range for inspection. Ideally, the only effect of cesiation would be to lower the work function. In practice, however, one finds that cesiation also tends to smear out structure in the spectra. We have found it advantageous to use the technique of higher-derivative spectroscopy[10] in order to enhance the structure and suppress the smooth background. In summary, our emphasis in this paper will be upon the presentation of higher-derivative spectra on cesiated samples.

In Sec. II we describe the experimental technique and the details of sample preparation. In Sec. III we present the results for Rh, Ir, Ni, Pd, and Pt and compare them with each other and with data on cesiated Cu and Au. One of our main concerns will be the identification of certain pieces of structure from one metal to the next. Sec. IV contains a summary of the data in the form of structure plots and a brief discussion in terms of the resonance picture of *d*-band metals. In a final part of Sec. IV, we offer some evidence and speculation concerning nondirect transitions with particular reference to an interesting energy region in Ir and Rh.

II. EXPERIMENTAL DETAILS

A. Apparatus

The photoemission experiments were carried out in a stainless steel ultrahigh vacuum chamber built earlier by Smith and Spicer[11] but modified to incorporate a 2 kW electron-gun evaporator and a spherical-diode retarding-potential-type energy analyzer. The system is shown schematically in Fig. 1. The disk-shaped emitter could be lowered, by means of a bellows-operated linear motion, from its energy-analysis position (A) out through a slot in the bottom of the spherical-collector can. During the lower part of the linear travel a cam-and-stop arrangement pivots the emitter-support arm to bring the emitter surface into the nearly horizontal postion (C) for electron-gun evaporation from a high-purity melt, or into the position (B) for cesiation.

The light was admitted into the chamber through a LiF window and was incident normally upon the sample surface. At the lower frequencies ($\hbar\omega < 6.3$ eV) we used a quartz-prism monochromator and a 1000-W Xenon arc source. At the higher photon energies ($\hbar\omega > 6.0$ eV), we used a McPherson model No. 225 monochromator and a Hinteregger-type hydrogen lamp modified to work in the hot-filament mode described by Eastman and Donelon.[12] The following modification to their design was found to be advantageous. By connecting a 100-kΩ 2-W resistor between the hot filament and the aluminum body of the original cathode, we found that large

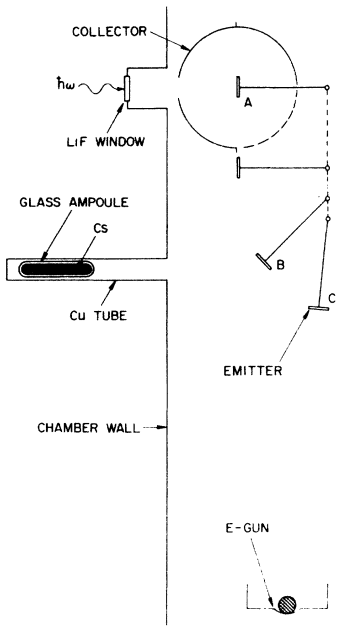

FIG. 1. Schematic diagram of the ultrahigh vacuum chamber showing the three alternative positions for the sample: *A* for photoemission measurements, *B* for cesiation, and *C* for sample deposition.

arc-discharge currents could be obtained for smaller filament emission. Direct connection of the filament to the cathode would result in the return of about one-half the thermionically emitted electrons to the filament with a consequent loss in discharge current. Complete isolation of the filament, on the other hand, led to difficult start-up and erratic discharge conditions.

The detection circuit used in these measurements was similar, in principle, to Eden's refinement[13] of the ac-modulation technique of Spicer and Berglund.[14] We have made several modifications, and our present circuit is illustrated schematically in Fig. 2. The retarding voltage V is produced by a ramp generator. The sinusoidal ac modulating voltage v is taken from a Wavetek model-111 function generator. The two voltages are added by means of an operational amplifier circuit, and the sum $V+v$ is applied across the capacitive bridge shown in Fig. 2. One arm of the bridge contains the experimental photodiode, whose capacitance we denote by C_p. The other arm contains a capacitor C and an inverting operational amplifier with an adjustable voltage gain α. The center-tapped transformer of the Eden circuit (and any-distortions associated therewith) have therefore been eliminated. Both the amplitude and phase of the inverting amplifier can be adjusted, and we find that the capacitive balance condition $\alpha = C_p/C$ can be achieved more easily and more precisely than by the conventional mechanical adjustment of a variable capacitor. At balance, only the ac modulated photocurrent is seen by the detector. The detector itself is a specially designed high-speed current-to-voltage transducer (designated I-V in Fig. 2) built around a Philbrick-Nexus field-effect-transistor operational amplifier. This detector replaces the Keithley model No. 417 picoammeter of the Eden circuit and can be built for a fraction of the cost. Its larger bandwidth permits operation at higher frequencies than with the Keithley model No. 417. This has advantages in the detection of higher harmonics as in higher-derivative spectroscopy.

The detector signal is fed into a Princeton Applied Research model No. HR-8 lock-in amplifier which derives its reference from the Wavetek function generator. Rather than use the sine wave, however, we used, for the lock-in reference, the synchronous square-wave output produced by the Wavetek. By simply tuning the reference channel of the HR-8 to the various harmonics of the square wave, we were able to examine the corresponding harmonics of the ac part of the photocurrent. Most of the spectra presented below are recordings of the amplitude of the third harmonic of the ac photocurrent. To first approximation, this is proportional to the second derivative of the photoelectron energy distribution curve (EDC). It was found that the tuned amplifiers in the input and reference channels of the HR-8 lock-in amplifier were sufficiently selective to isolate the harmonic under consideration, provided the frequency was not too low. The fundamental frequency used in these investigations was typically 57 Hz with the third harmonic occurring at 171 Hz. Frequencies as high as 1 kHz, however, were found to be quite practical.

B. Sample preparation

The substrate upon which the transition-metal films were deposited was a highly polished copper disk. The base pressures were in the 50–200-pTorr range. Pressures rose typically to 5×10^{-8}

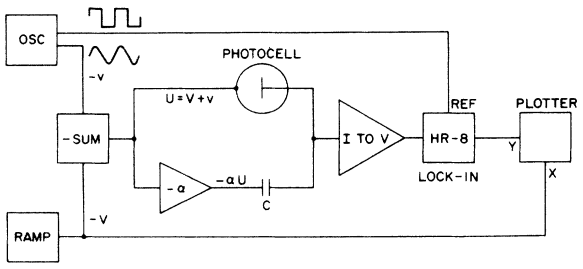

FIG. 2. Bridge circuit used in the detection of the ac photocurrent and its higher harmonics.

Torr during the electron-gun evaporation, fell to below 5×10^{-9} Torr within 1 min after evaporation, and regained base values within about an hour. The purities of the melts were better than 99.99%. Photoemission spectra were measured on the clean samples, and after it had been established that the results reproduced those of previous experiments, we proceeded with the cesiation. In the case of Ir, where it appears that no previous measurements have been reported on either clean or cesiated samples, we took extensive data prior to cesiation.

The cesiations were performed in the same way as in previous work on the noble metals.[15,16] The ampule containing 99.99%-purity Cs shown in Fig. 1 was kept intact until after bakeout of the vacuum system. It was then broken open, and heated gently from outside when Cs was required. At first, sparing amounts of Cs were deposited on the sample, and the lowering of the work function was monitored by measuring the EDC's at one or two photon energies. It was found, however, that the best results were obtained after large quantities of Cs had been admitted into the vacuum chamber, thereby cesiating its internal parts and equalizing their work functions.[17] In this equalization-of-work-function effect, the surfaces of particular importance were the inside of the spherical-collector electrode and the sides of the emitter disk and its supporting rod. In order to accelerate the equalization-of-work-function effect, we found it expedient to use the emitter disk itself to transport sufficient quantities of Cs up into the collector sphere. This was accomplished by cooling the emitter by means of liquid nitrogen, and then depositing thick films of Cs (recognizable by their characteristic golden color) upon it. The chamber pressure would rise to about 1×10^{-8} Torr during this process. The emitter was then raised to a position within the collector and allowed to warm up to room temperature. Usually, the system would be left overnight, by which time all the Cs detectable to the unaided eye had evaporated. Measurements of the EDC's were taken at this point. The equal-work-function condition was recognizable when the low-energy cutoff of the EDC was sharp and occurred at zero retarding voltage.

Fresh samples of transition metal were then evaporated over the earlier samples. At this stage, several things could happen, depending on how much Cs had been released into the chamber in the previous operations, described above. In some cases, we were able to retrieve almost completely the spectra characteristic of the clean material. It would then be necessary to recesiate the sample. In other experiments, the newly evaporated sample would be observed to cesiate spontaneously, but gradually. This was observed as a progressive lowering of the work function with time. At the other extreme, we found that some newly evaporated samples would be fully cesiated before their spectra could be measured.

In general, we found that samples with lesser amounts of cesium, particularly those not recesiated, tended to show sharper photoemission spectra, but often at the expense of a higher work function.

III. RESULTS AND COMPARISONS

A. Clean and cesiated samples

In Fig. 3 we show, for each of the metals Rh, Ir, Pd, and Pt, an EDC taken on a clean and on a fully cesiated sample. Following the usual convention, the curves are referred to the initial-state energy by plotting them against $E = E' - \hbar\omega + \Phi$, where E' is the kinetic energy in vacuum and Φ is the work function. The zero of energy then represents the Fermi level ($E = E_F = 0$).

The EDC's on clean Pt and Pd are in good agreement with those obtained by Lin *et al.*[2] and by Janak *et al.*,[4] respectively. The EDC on clean Rh is similar to, but not identical with, that of Pierce and Spicer.[3] The first few evaporations of Rh produced spectra in close agreement with those of Pierce and Spicer. Subsequent evaporations within the same experimental run (presumably under

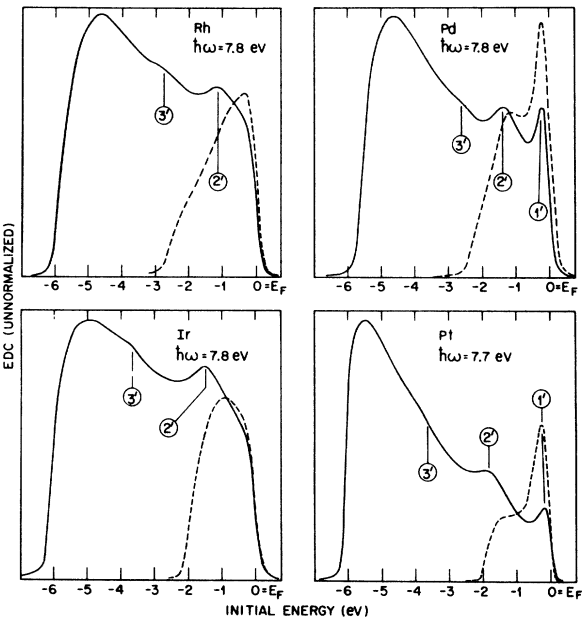

FIG. 3. Photoelectron energy spectra taken on both clean (dashed curves) and cesiated (full curves) samples of Rh, Pd, Ir, and Pt. The spectra are referred to initial-state energy E ($=E' - \hbar\omega + \Phi$) which places the zero of energy at the Fermi level E_F.

cleaner conditions, since the electron-gun had been given an opportunity to outgas itself more thoroughly) produced spectra like that in Fig. 3, in which the piece of structure which appears prominently at -1.1 eV in the Pierce-Spicer spectrum appears less prominent and is obscured by the behavior in the threshold region.

The spectra, shown in Fig. 3, on cesiated samples of Pd and Pt show that the leading peak just below E_F, (labeled 1), seen in the clean samples, is preserved in the cesiated samples and that additional structure (labeled 2′ and 3′) is revealed at lower energies. The spectra on cesiated Rh and Ir are similar to those on Pd and Pt except that the prominent peak just below E_F is missing. This is not unexpected, since Rh and Ir have one less electron per atom than Pd and Pt and the Fermi level will consequently fall at a lower energy with respect to the top of the d bands. Note that the spacing of the structures labeled 2′ and 3′ is greater for Ir and Pt than for Rh and Pd. This is to be expected since the d bands for the $5d$ metals are thought to be wider than for the $4d$ metals. Similarly, we note from Fig. 3 that the d bands in the nine-electrons-per-atom metals, Rh and Ir, are wider than in the ten-electrons-per-atom metals Pd and Pt. The spectra therefore fix the relative d-band widths. This point is expanded upon in considerable detail below and in the following paper[1] of this series.

At higher photon energies, additional structure is seen in the clean spectra. It was confirmed that the same structure occurred in the cesiated spectra. This provides some check that the Cs on the surface is not itself interfering with the spectral information. The peaks seen in the cesiated spectra of Fig. 3 at about 1 eV above the low-energy cutoff are attributed to electrons which have undergone an inelastic scattering before emerging from the metal. These peaks will be ignored in subsequent band-structure interpretations.

B. EDC and its second derivative

In Fig. 4 we show the results obtained on cesiated Pt at $\hbar\omega = 8.8$ eV. The EDC, $N(E, \hbar\omega)$, and the negative of its second derivative, with respect to initial energy, $-N''(E, \hbar\omega)$, are both shown. More precisely, the curve labeled a is the amplitude of the first harmonic of the ac photocurrent and curve b is the negative of the amplitude of the third harmonic, both plotted against retarding voltage or, equivalently, the electron energy. It is seen that the weak structure in the EDC is considerably enhanced in the derivative curve. Much of the presentation below and the analysis in the following paper will be based upon derivative spectra like that shown in Fig. 4. It should be borne in mind, therefore, that we will frequently be talking about rather subtle structure on the actual EDC and be neglecting an appreciable background.

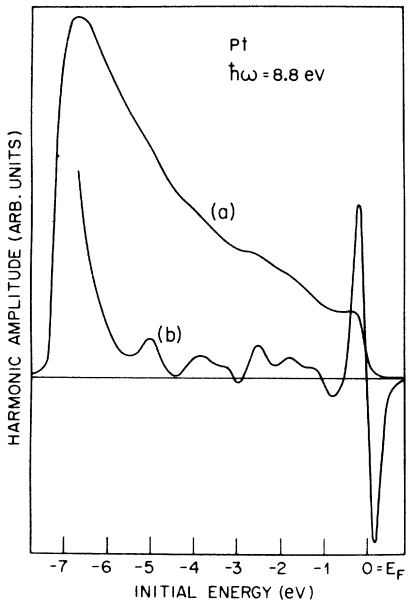

FIG. 4. Photoemission spectra measured on cesiated Pt at $\hbar\omega = 8.8$ eV. Curve a is the amplitude of the first harmonic of the ac photocurrent corresponding to the photoelectron energy distribution curve, $N(E, \hbar\omega)$; curve b is the negative of the amplitude of the third harmonic corresponding to the minus the second derivative spectrum, $-N''(E, \hbar\omega)$.

C. Platinum and gold

A set of derivative spectra taken on cesiated Pt at various photon energies is shown in Fig. 5. As in Figs. 3 and 4, we see a peak just below the Fermi energy and additional structure in the d-band region. This structure is quite rich and varies quite markedly with photon energy. The changes in profile of the spectrum on cesiated Pt are very similar to those reported earlier on cesiated Au[16] a selection of which we show in Fig. 6. Specific features of the Pt spectra of Fig. 5, also seen in the Au spectra of Fig. 6, are listed below.

Feature (i). At the lower photon energies we observe a peak labeled 1′. As $\hbar\omega$ is increased, this peak splits into the doublet $1a$ and $1b$. This occurs at about $\hbar\omega = 8.4$ eV in Au and at about $\hbar\omega = 9.2$ eV in Pt. The higher-energy component, labeled $1a$, remains at the same initial energy as 1′. The lower component $1b$ moves to lower initial energies as $\hbar\omega$ is increased. This splitting can be seen in the EDC's also, and has been remarked upon by Lin *et al.*[2]

Feature (ii). A structural feature labeled 2′ is observable as a single prominent peak in Pt at

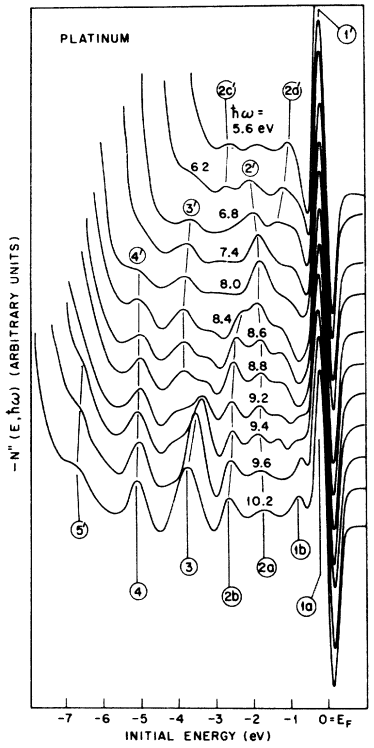

FIG. 5. Higher derivative photoemission spectra, $-N''(E,\hbar\omega)$, for cesiated Pt.

$\hbar\omega = 8.0$ eV, and in Au at $\hbar\omega = 7.6$ eV. On increasing $\hbar\omega$, this peak splits into the doublet labeled $2a$ and $2b$. In Figs. 5 and 6, the first appearance of component $2b$ is observed at $\hbar\omega = 8.4$ eV in Pt and at $\hbar\omega = 7.8$ eV in Au.

Feature (iii). If the same structural feature labeled $2'$ discussed in (ii) is pursued to lower photon energies, it is observed to move to lower initial energies and also to undergo further profile changes. A shoulder emerges on the high-energy side and eventually becomes the peak labeled $2a'$. At sufficiently low photon energies, a peak emerges on the low-energy side which we have labeled $2c'$. The central component retains the label $2'$.

Feature (iv). A peak labeled $3'$ in the Pt spectra of Fig. 5 is observed to move downwards slightly in initial energy as $\hbar\omega$ is increased from 6.8 to 8.8 eV. A similar feature is seen in the Au spectra of Fig. 6 between $\hbar\omega = 7.4$ eV and $\hbar\omega = 8.4$ eV. On further increasing $\hbar\omega$, peak $3'$ becomes obscured by the abrupt emergence of a peak labeled 3 at a slightly higher initial energy. This event can be seen in the curve for $\hbar\omega = 9.4$ eV for Pt in Fig. 5 and for $\hbar\omega = 8.6$ eV for Au in Fig. 6.

Feature (v). A piece of structure labeled $4'$ is observed in both Pt and Au at initial energies below those of peak $3'$.

In summary, the "sequence of events" in the evolution of the profile of the spectrum on varying $\hbar\omega$ in Pt is very similar to that in Au. The numbering system of the peaks has been arranged so as to bring out this similarity. This system has been applied uniformly throughout this paper in order to indicate our identifications of structure from one metal to the next. We should therefore mention that, in the case of Au, our numbering of peaks differs from that used in a previous paper. Peaks 1, 2, 3, 4, 5, 6, and $5a$ of Ref. 16 correspond, respectively, to peaks $1a$, $1b$, $2a$, $2b$, 3, $4'$ and $3'$ of this paper. Peaks $3a$, $3b$, and $3c$ of Ref. 16 correspond to peaks $2a'$, $2'$, and $2c'$ of this paper, respectively.

In addition to the major points, feature (i)–(v) above, we note the following minor points. These are features of the spectra which are worthy of mention, but which have not been relied upon heavily in the analysis of this and the following paper.

Feature (vi). In Fig. 5 we note a shoulder labeled $5'$. A hint of this is seen also in Au in Fig. 6, and more clearly in the spectra of Ref. 16.

Feature (vii). At $\hbar\omega = 9.4$ in the Pt spectra of Fig. 5 we observe a piece of structure between peaks $1b$ and $2a$ having an initial energy of about -1.3 eV. A similar feature is seen in the Au of Fig. 6 at $\hbar\omega = 8.0$, 8.2, and 8.4 eV.

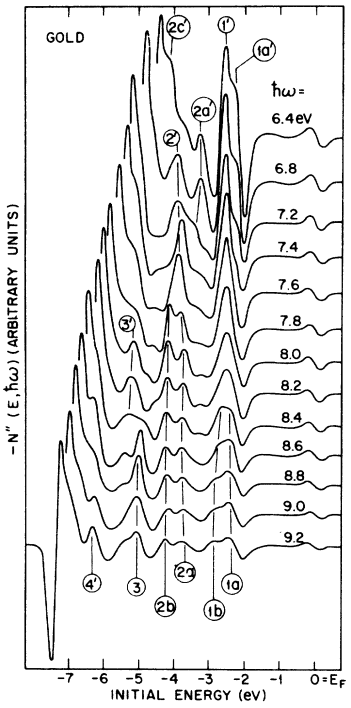

FIG. 6. Higher derivative photoemission spectra, $-N''(E,\hbar\omega)$, for cesiated Au (taken from Ref. 16).

We emphasize here a danger in attaching too much significance to rather weak pieces of structure in the derivative spectra. It is readily shown that two sharp neighboring peaks in the EDC, $N(E, \hbar\omega)$, will give rise to two peaks in the $-N''(E, \hbar\omega)$ spectrum but will be accompanied by a spurious intermediate peak which arises simply through the differentiation process. Some of the weaker structures, such as those listed in (vi) and (vii), may originate in this way. We have therefore not relied on them too heavily in our interpretation, even though there are features in the calculated spectra (see following paper) to which they correspond.

D. Iridium, rhodium, and palladium

Sets of derivative spectra taken on cesiated samples of Ir, Rh, and Pd are shown for various photon energies in Figs. 7, 8, and 9, respectively. The structure in these curves is not as strong as in the Pt and Au spectra. However, several prominent pieces of structure are observed and the sequence of events, as $\hbar\omega$ is varied, is similar to that in Pt and Au. We have used the same uniform numbering system for the peaks to indicate our identifications.

In the Ir spectra of Fig. 7, we see a peak labeled 2′ at $\hbar\omega = 6.4$ eV. On increasing $\hbar\omega$, this peak moves to slightly higher initial energies and eventually evolves into the doublet 2*a* and 2*b*, just as in Pt and Au. The peak 3′ is also observed in Ir. It moves downwards slightly in initial energy as $\hbar\omega$ is increased and is eventually obscured by the growth of peak 3, observable in the curve for $\hbar\omega = 11.0$ eV. A peak 4′ is observable at energies below 3′. Similar features are seen in the curves for Rh and Pd in Figs. 8 and 9, respectively, and have been labeled accordingly.

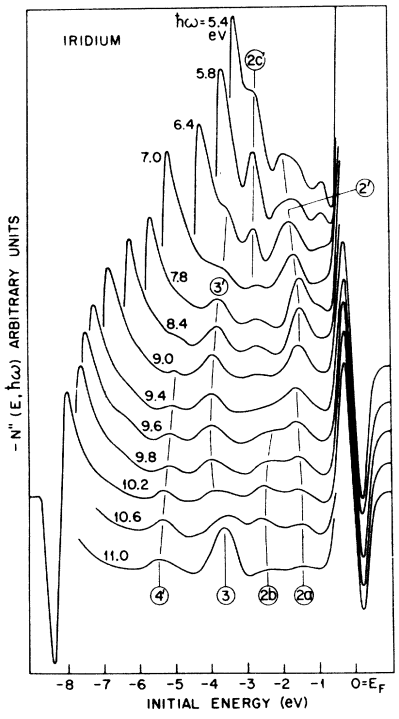

FIG. 7. Higher derivative photoemission spectra, $-N''(E, \hbar\omega)$, for cesiated Ir.

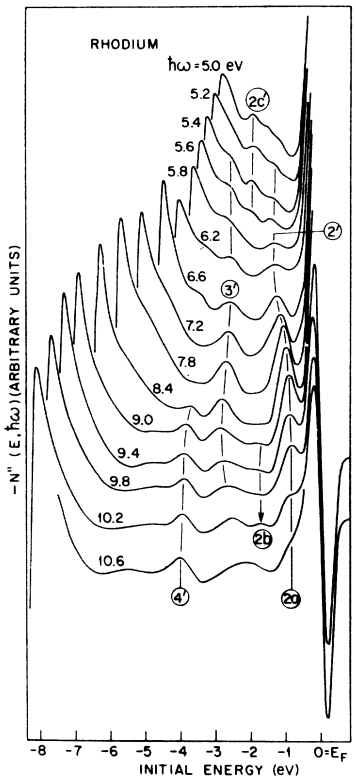

FIG. 8. Higher derivative photoemission spectra, $-N''(E, \hbar\omega)$, for cesiated Rh.

The peak just below the Fermi level labeled 1, observed in Pt and Pd, has not been so labeled in Rh and Ir. The peak just below E_F in the derivative spectra of Figs. 7 and 8 is a consequence of the precipitous *edge* in the EDC at the Einstein limit and is therefore an artifact of the Fermi cutoff. It is not to be associated, as in Pt and Pd, with a peak in the density of states or the energy distribution of the joint density of states. In the cases of Pt and Pd, the peak just below E_F was observed not just in the $-N''(E, \hbar\omega)$ spectrum but also in the $N(E, \hbar\omega)$ spectrum (see Fig. 3).

No consistent procedure for normalizing the spectra has been adopted. The vertical scales have been chosen mainly for ease in drawing the figures. Also the sharpness of structure was found

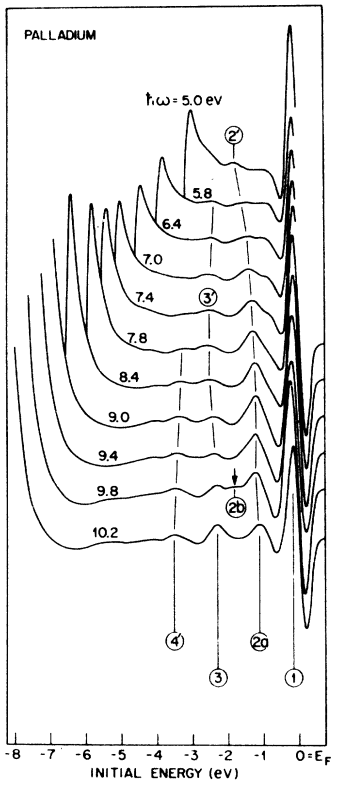

FIG. 9. Higher derivative photoemission spectra, $-N''(E,\hbar\omega)$, for cesiated Pd.

to vary with the details of the cesiation procedure and is therefore sample dependent. The spectra on cesiated Au in Fig. 6 represent a case where the structure was quite pronounced. The spectra on cesiated Pd in Fig. 9, on the other hand, represent a situation in which the sample had been well cesiated, and the structure appears weaker. Samples of Pd more lightly cesiated than that in Fig. 9 showed stronger structure.

To summarize up to this point, we have observed that the profile of the photoelectron energy spectrum varies with $\hbar\omega$ in a very similar way for Pt, Au, Ir, Rh, and Pd. Specific identifications of structure from metal to metal have been made. One of the most ubiquitous profile changes in these metals is the sudden emergence of peak 3 at a critical photon energy. The first observation of this feature appears to be that of Yu and Spicer[8] in their early work on Pd. Yu and Spicer interpreted this feature as a direct transition effect. Their interpretation is confirmed and considerably elaborated upon in the following paper.

E. Nickel and copper

Spectra on clean and cesiated Ni have also been measured as part of this work. Derivative spectra on cesiated samples will be presented and discussed below. Before considering Ni, however, an instructive preliminary is to examine the spectra taken on cesiated samples of the neighboring $3d$ metal, Cu. Although cesiated Cu has been examined and discussed previously by several workers,[10,15,18] it has not been possible until now to establish the identifications between the structures seen in the Cu spectra and those seen in the other fcc d-band metals. Since such identifications are a major theme of this paper, we will present the identifications for Cu here.

Figure 10 shows the derivative spectra taken on cesiated Cu in the photon energy range $7.4 < \hbar\omega < 8.4$ eV. As remarked upon elsewhere,[15] this is a very interesting range, since the profile varies rather rapidly with $\hbar\omega$. The spectra of Fig. 10, taken with the better resolution of the spherical geometry, supersede those presented earlier[10,15] using the relatively low resolution of cylindrical geometry.

We note in Fig. 10 the same familiar features listed in Sec. III C. Peak $2'$ evolves into the doublet $2a$ and $2b$, and peak $3'$ evolves into peak 3. The Cu spectra, therefore, fit the consistent pattern of behavior noted for Pt, Au, Ir, Rh, and Pd.

Turning now to Ni, we present in Fig. 11, derivative spectra taken on cesiated Ni in the photon energy range 4.8–9.0 eV. Although taken in the same measuring apparatus, the structure is con-

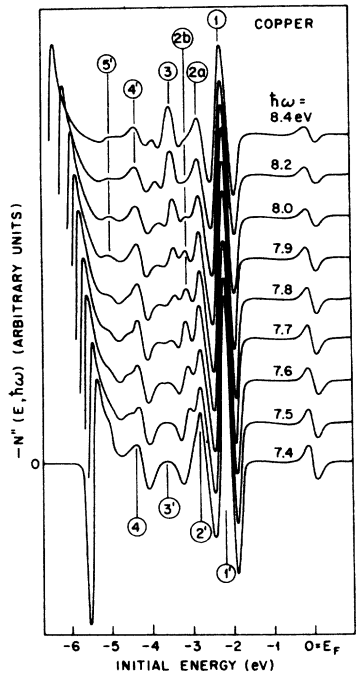

FIG. 10. Higher derivative photoemission spectra, $-N''(E,\hbar\omega)$, for cesiated Cu.

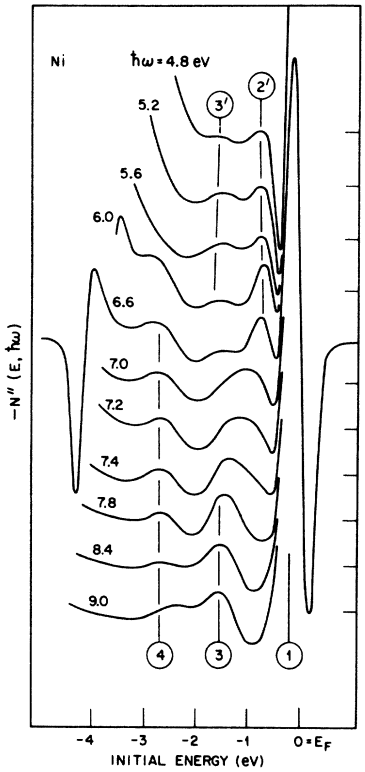

FIG. 11. Higher derivative photoemission spectra, $-N''(E,\hbar\omega)$, for cesiated Ni.

siderably less rich than in Cu. There are, however, some vestiges of the behavior seen in Cu and the other metals, and the peaks in Fig. 11 have been labeled according to our current identifications. At the lower photon energies, two peaks labeled 2′ and 3′ are observed. These are discernible in the EDC's on cesiated Ni reported by Callcott and MacRae.[7] (In that paper, they are labeled 2*a* and 2*b*, respectively.) At $\hbar\omega = 7.0$ eV, peak 3′ is no longer seen, and peak 2′ appears to have broadened. On increasing $\hbar\omega$, the weight of this broader piece of structure moves downwards in initial energy. We attribute this to the emergence of peak 3 as in the other metals. Peak 2′, however, does not evolve into peaks 2*a* and 2*b* as in the other metals. At the higher photon energies, peak 3 tends to coalesce with peak 4. These two features correspond, in the EDC's on clean Ni obtained by Pierce and Spicer,[5] to the rather broad single peak centered at about 2 eV below E_F.

If one compares the spacings between the peaks in the Ni spectra of Fig. 11 with the corresponding spacings in the Cu spectra, one concludes that the width of the *d* band in Ni is only (10–20)% wider than that in Cu. Our results are therefore in accord with those of Eastman[19] using higher photon energies, and those of Hüfner *et al.*[20] using x-ray-photoelectron spectroscopy. There it was found that the measured *d*-band width was appreciably narrower than that predicted by the generally accepted first-principles band calculations.[21]

The lack of structural resolution in the Ni spectra compared with those of Cu, may be associated with the occurrence, in the former, of ferromagnetism. In the x-ray-photoemission work reported by Hüfner *et al.*,[20] it was found that the Ni spectrum could be reproduced fairly well, in both its over-all width and general featurelessness, simply by adding two Cu *d*-band densities of states rigidly shifted with respect to each other by an exchange splitting of 0.3 eV. The featurelessness came about through a fortuitous canceling between peaks in the density of states for one spin band and valleys in the other, and vice-versa. A similar effect may be responsible for the relative lack of structure in the Ni photoemission spectra at lower photon energies.

IV. SUMMARY AND DISCUSSION

A. Structure of *d* bands

Our experimental results on Rh, Ir, Ni, Pd Pt, Cu, Ag, and Au, including the selection presented above and work presented elsewhere,[15,16] are summarized in the structure plots of Fig. 12. The figure shows the initial energy location of peaks (full circles) and shoulders (open circles) in the derivative spectra for a range of photon energies. The full lines connecting some of the points have no theoretical significance. They are intended only to trace the loci of important structures in the E, $\hbar\omega$ plane. The lines are numbered according to the identifications made above.

The first observation we make is that the peak loci numbered in Fig. 12 tend to be fairly horizontal. In this regard, they have "initial-state character" and are related to the structure of the occupied *d* bands. A detailed comparison with model band calculations will be made in the following paper. The important point we wish to make here is that the main features of the pattern of the structure plot appear consistently from metal to metal. As far as we know, this consistency of pattern is not apparent in any previous data and has emerged only after our measurements on cesiated samples.

A further observation is that the *d*-band pattern of one plot can, to a good approximation, be obtained from another by a uniform shifting and stretching of the vertical scale. This is in accord with the principal result of the resonance formulation of *d*-band metals.[22] In the resonance formulation, the main features of the *d* bands are related to the properties of a singularity in the tangent of the $l = 2$ phase shift. This "resonance" is characterized by two parameters, namely, its position and its width. Once these have been specified, the

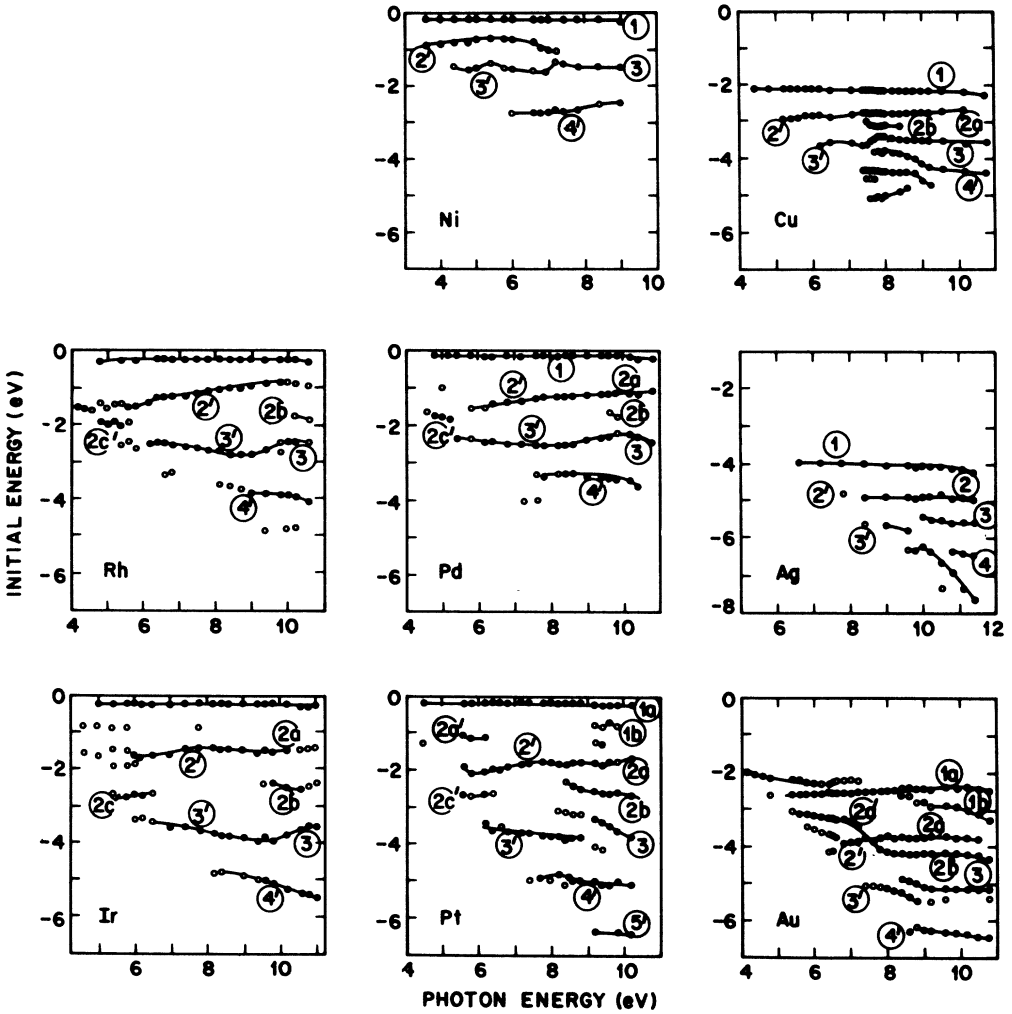

FIG. 12. Structure plots summarizing the experimental photoemission spectra of Rh, Ir, Ni, Pd, Pt, Cu, Ag, and Au. Full and open circles represent peaks and shoulders in the measured derivative spectra $-N''(E,\hbar\omega)$. The full lines trace the loci of prominent structures.

d bands are almost completely determined and their internal features, although complicated, should be the same for metals of the same crystal structure. In a previous paper,[23] we have offered the experimental results as the first direct experimental confirmation of this principal result of the resonance picture. The plots of Fig. 12 are arranged as the metals appear in the Periodic Table. It is seen that the width of the *d* bands increases as one either (a) moves down a column, or (b) moves from right to left along a row in the figure. In making comparisons of this kind, we should repeat that the peaks in Ir and Rh at about -0.2 eV should be disregarded since they are a consequence of the precipitous Fermi *edge* and are not to be identified with any peak in the density of states or energy distribution of the joint density of states.

B. Unoccupied bands

In comparing the plots of Fig. 12, we note that, in addition to the width and position of the *d* resonance, there is a third important parameter, namely, the location of the pattern with respect to the $\hbar\omega$ scale. Certain events in the evolution of the spectral profile take place at different photon energies for different metals. This is readily explained by variations in the relative position of the unoccupied bands. For example, if the unoccupied bands were raised to higher energies, optical transitions giving rise to a given event in the evolution of the photoemission spectrum would still occur, but at higher photon energies. In other words, the pattern of plots such as those in Fig. 12 would be shifted to the right.

Let us focus here on two specific events, namely,

the emergence of peaks 2*b* and 3. The former event is seen clearly in Cu, Au, Pt, and Ir, it is just discernible in Rh and Pd, and it is not observed in Ni or Ag. In the following paper, it is proposed that these two events represent the onset of transitions to states near the minimum of band 7, which becomes available as a source of final states at some critical photon energy. If we make a closer inspection of the plot for Au in Fig. 12, we find that these two events fall close to a line on the plot of slope equal to -1 and whose equation is given by

$$E_f = E + \hbar\omega = 3.6 \text{ eV},$$

where E_f $(= E' + \Phi)$ denotes the final-state energy referenced to E_F. Clearly such a line corresponds to optical transitions to states of constant final energy. We therefore place the minimum of band 7 in Au at about 3.6 eV above the Fermi level. As it turns out (see following paper), band 7 is quite flat in the region of its minimum, and the minimum itself occurs quite close in energy to the plane-wave-like level L_1. Therefore, to within one- or two-tenths of an eV, we can place L_1 also at about 3.6 eV above E_F. A similar inspection of the Cu plot leads us to place L_1 in Cu at about 4.3 eV above E_F. These locations of L_1 above E_F in Au and Cu are quite close to the alternative estimates of 3.5 and 4.05 eV, respectively, obtained from a careful analysis[16,24] of the rectangular-box feature[25] in the photoemission spectra associated with conduction-band–to–conduction-band transitions near $L_2, \rightarrow L_1$. This lends support to our analysis of peaks 2*b* and 3 and indicates that it can be applied with confidence to the other metals.

In Rh, Pd, Pt, and Ir, the emergence of peaks 2*b* and 3 leads us to place the minimum of band 7 and the level L_1 at about 8.5, 8.0, 6.1, and 7.1 eV above E_F, respectively. The estimated error is ± 0.2 eV. In the case of Ni, peak 2*b* is not observed and, in Fig. 11, the photon energy at which the peak we have identified as 3, emerges is not well defined. Our estimate in Ni is therefore more tentative. We place L_1 in Ni at 5.7 ± 0.4 eV above E_F.

C. Nondirect transitions in Ir and Rh

In the comparisons above, we have been concerned with those features of the spectra which are consistent with one-electron band theory. The predictions of one-electron band theory are calculated in the following paper, and it will be shown that the predicted pattern of behavior is very similar to that observed in the experimental spectra. Indeed, this similarity has been used to generate empirical band structures.[23] Since our emphasis in the following paper will be on those aspects of the spectra consistent with direct transitions in a one-electron band model, it is appropriate to present some discussion here of those features of the spectra which are in definite disagreement.

One point of disagreement concerns the strength of structure. In Fig. 13, we present some EDC's taken on clean Ir at various photon energies. For comparison, we show in Fig. 14 the results of some calculations of the energy distribution of the joint density of states (EDJDOS). As discussed elsewhere[15,23,1] this is a property of the band structure representing the phase space available for optical transitions as a function of E and $\hbar\omega$. Apart from modulation by momentum matrix elements and scattering and escape factors,[26] one expects the EDJDOS to bear a resemblance to the EDC.[15] The calculations were performed with a model band structure obtained previously[23] by shifting and stretching the *d* bands of Burdick's APW calculation[27] on Cu. A Lorentzian broadening of 0.2-eV full width at half-maximum (FWHM) has been introduced. Nevertheless, the calculated spectra are much sharper than the measured spectra. The explanation for this is not yet clear. The discrepancy is likely to be due in part to purely experimental factors such as finite instrumental resolution and imperfect sample and surface control. It should be pointed out that Ir represents

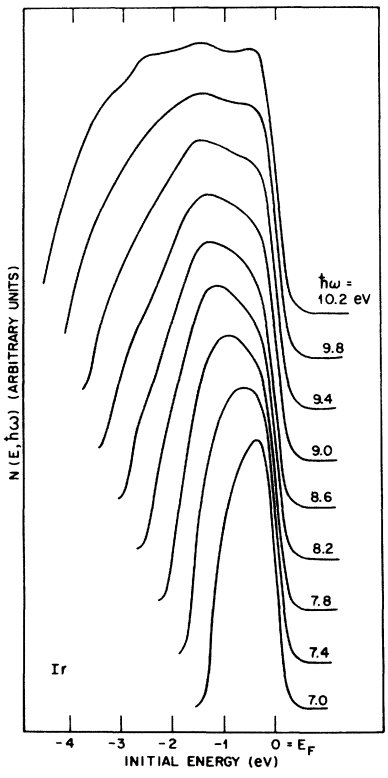

FIG. 13. Photoelectron energy spectra, $N(E, \hbar\omega)$ measured on clean Ir.

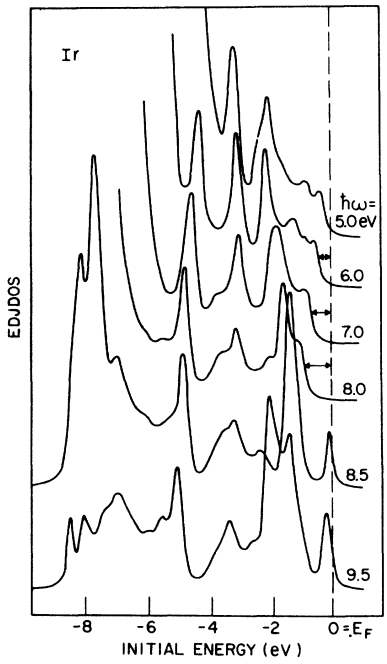

FIG. 14. The energy distribution of the joint density of states (EDJDOS) for Ir calculated from a model band structure (Ref. 23) and convolved with a Lorentzian broadening function having 0.2-eV FWHM. The double-ended horizontal arrows represent an energy range close to E_F in which direct transitions are forbidden (i.e., the unbroadened EDJDOS is zero).

an extreme case as far as the lack of sharpness is concerned. Improvements in sample preparation may ultimately produce sharper spectra. On the other hand, the lack of sharpness may be an intrinsic effect due to a large background arising from either (a) nondirect transitions,[28,29] (b) scattered electrons, (c) the surface-plasmon-mediated surface photoelectric effect,[30] or (d) emission from surface states.[31]

There is another, and perhaps more significant, discrepancy in Ir between the experimental spectra and the direct transition model. This concerns the location of the upper edge of the spectrum. Starting at about $\hbar\omega = 5.0$ eV, the upper edge of the spectrum is predicted to move downwards in initial energy as $\hbar\omega$ is increased. The calculations predict an absence of photoelectrons in the energy range indicated by the double-ended horizontal arrows in Fig. 14. (The tail of the curve in this region is a consequence of the Lorentzian broadening. The EDJDOS itself vanishes completely in this region.) Eventually, at high enough photon energy, a peak is predicted to appear just below E_F. This is seen in the curve for $\hbar\omega = 8.5$ eV in Fig. 14. The situation here is somewhat reminiscent of that which occurs in some of the semiconductors. For example, in GaAs,[32] the valence-band maximum is at Γ. Optical transitions from the top of the valence band can occur only at those photon energies for which there is a final state available at Γ. At all other photon energies the upper edge of the EDC occurs at a lower initial energy. Similarly, there is in Ir an area close to E_F in the $E, \hbar\omega$ plane for which no direct transitions are possible. Turning to Fig. 13, we see, in contradiction to the prediction, that the edge of the EDC is quite stationary. This is found also in the derivative spectra on both clean and cesiated samples. The photoelectrons observed in the forbidden energy range must therefore be categorized as nondirect. We are adopting here a rather broad definition of the nondirect transition. It would cover not only the specific nondirect mechanism of Spicer[28] and Doniach,[29] but would embrace also the surface photoelectric mechanisms proposed by Endriz and Spicer,[30] as well as the emission from surface states proposed by Schaich and Ashcroft[31] and observed in W by Waclawski and Plummer[33] and by Feuerbacher and Fitton.[34] We should also bear in mind the possibility of imperfect sample or surface preparation. The existence of the forbidden range (zero EDJDOS) appears to be an inevitable consequence of a direct transition calculation on Ir or Rh. (A similar discrepancy not discussed in detail here is also found for the upper edge in Rh.) The Fermi energy is pinned quite precisely with respect to the top of the d bands by the requirements that there be nine occupied electron states per atom and that the Fermi surface topology be correct.[35] The unoccupied bands are known with less certainty. However, any permissible adjustment of the upper bands would merely shift the position of the forbidden region with respect to the photon energy scale. We conclude that, whatever the ultimate explanation, this forbidden energy range in Ir and Rh provides a promising region in which to pursue experimentally some of the interesting possibilities listed above.

[1]N. V. Smith and L. F. Mattheiss, preceding paper, Phys. Rev. B 9, 1341 (1973): N.V. Smith, following paper, Phys. Rev. B 9, 1365 (1973).
[2]S. F. Lin, D. T. Pierce, and W. E. Spicer, Phys. Rev. B 4, 326 (1971).
[3]D. T. Pierce and W. E. Spicer, Phys. Rev. B 5, 2125 (1972).
[4]J. F. Janak, D. E. Eastman, and A. R. Williams, Solid State Commun. 8, 271 (1970).
[5]D. T. Pierce and W. E. Spicer, Phys. Rev. Lett. 25, 581 (1970).
[6]D. E. Eastman and W. F. Krolikowski, Phys. Rev.

Lett. 21, 623 (1968).
[7]T. A. Callcott and A. U. MacRae, Phys. Rev. 178, 966 (1969).
[8]A. Y-C. Yu and W. E. Spicer, Phys. Rev. 169, 497 (1968).
[9]A. Y-C. Yu, Ph.D dissertation (Stanford University, 1967) (unpublished); R. C. Vehse, E. T. Arakawa, and M. W. Williams, Phys. Rev. B 1, 517 (1970); A. J. Blodgett, Jr. and W. E. Spicer, Phys. Rev. 146, 390 (1966); R. C. Vehse and E. T. Arakawa, Phys. Rev. 180, 695 (1969).
[10]N. V. Smith and M. M. Traum, Phys. Rev. Lett. 25, 1017 (1970).
[11]N. V. Smith and W. E. Spicer, Phys. Rev. 188, 593 (1969).
[12]D. E. Eastman and J. J. Donelon, Rev. Sci. Instrum. 41, 1648 (1970).
[13]R. C. Eden, Rev. Sci. Instrum. 41, 252 (1970).
[14]W. E. Spicer and C. N. Berglund, Rev. Sci. Instrum. 35, 1665 (1964).
[15]N. V. Smith, Phys. Rev. B 3, 1862 (1971).
[16]N. V. Smith, Phys. Rev. B 5, 1192 (1972).
[17]I. Lindau and L. Walldén have commented on a similar effect in Phys. Scripta, 3, 77 (1971).
[18]N. V. Smith, Phys. Rev. Lett. 23, 1452 (1969); I. Lindau and L. Walldén, Solid State Commun. 9, 209 (1971).
[19]D. E. Eastman in *Techniques of Metals Research*, edited by E. Passaglia (Interscience, New York, 1972), Vol. 6, Part 1, p. 411.
[20]S. Hüfner, G. K. Wertheim, N. V. Smith, and M. M. Traum, Solid State Commun. 11, 323 (1972).
[21]J. O. Dimmock in *Solid State Physics*, edited by H. Ehrenreich, F. Seitz, and D. Turnbull (Academic, London, 1971), Vol. 26, p. 103.
[22]J. M. Ziman, Proc. Phys. Soc. Lond. 86, 337 (1965); V. Heine, Phys. Rev. 153, 673 (1967); J. Hubbard, Proc. Phys. Soc. Lond. 92, 921 (1967); D. G. Pettifor, Phys. Rev. B 2, 3031 (1970).
[23]N. V. Smith and M. M. Traum, Phys. Rev. Lett. 29, 1243 (1972).
[24]I. Lindau and L. Walldén, Solid State Commun. 9, 1147 (1971).
[25]R. Y. Koyama and N. V. Smith, Phys. Rev. B 2, 3049 (1970).
[26]C. N. Berglund and W. E. Spicer, Phys. Rev. 136, A1030 (1964).
[27]G. A. Burdick, Phys. Rev. 129, 138 (1963).
[28]W. E. Spicer, Phys. Rev. 154, 385 (1967).
[29]S. Doniach, Phys. Rev. B 2, 3898 (1970).
[30]J. G. Endriz and W. E. Spicer, Phys. Rev. B 4, 4159 (1971).
[31]W. L. Schaich and N. W. Ashcroft, Phys. Rev. B 3, 2452 (1971).
[32]W. E. Spicer and R. C. Eden, in *Proceedings of the International Conference on the Physics of Semiconductors*, Moscow, 1968 (Publishing House Nauka, Leningrad, 1968), Vol. 1, p. 65.
[33]B. J. Waclawski and E. W. Plummer, Phys. Rev. Lett. 29, 783 (1972).
[34]B. Feuerbacher and B. Fitton, Phys. Rev. Lett. 29, 786 (1972).
[35]O. K. Andersen, Phys. Rev. B 2, 883 (1970).